Biomaterials 32 (2011) 1311–1316

Contents lists available at ScienceDirect

Biomaterials

journal homepage: www.elsevier.com/locate/biomaterials

Hyperbranched polyglycerols on the nanometer and micrometer scale

Dirk Steinhilber [a,1], Sebastian Seiffert [b,*,1], John A. Heyman [b,c], Florian Paulus [a], David A. Weitz [b,d], Rainer Haag [a,*]

[a] Free University Berlin, Institute for Chemistry and Biochemistry, Takustr. 3, D-14195 Berlin, Germany
[b] Harvard University, School of Engineering and Applied Sciences, 29 Oxford Street, Cambridge, MA 02138, USA
[c] HabSel, Inc., One Broadway, 14th Floor, Cambridge, MA 02142, USA
[d] Harvard University, Department of Physics and Kavli Institute for Bionano Science and Technology, 29 Oxford Street, Cambridge, MA 02138, USA

ARTICLE INFO

Article history:
Received 2 September 2010
Accepted 6 October 2010
Available online 2 November 2010

Keywords:
Biocompatibility
Cell encapsulation
Hydrogel
Microsphere
Nanoparticle

ABSTRACT

We report the preparation of polyglycerol particles on different length scales by extending the size of hyperbranched polyglycerols (3 nm) to nanogels (32 nm) and microgels (140 and 220 μm). We use miniemulsion templating for the preparation of nanogels and microfluidic templating for the preparation of microgels, which we obtain through a free-radical polymerization of hyperbranched polyglycerol decaacrylate and polyethylene glycol-diacrylate. The use of mild polymerization conditions allows yeast cells to be encapsulated into the resultant microgels with cell viabilities of approximately 30%.

1. Introduction

Polymer therapeutics [1,2] and tissue engineering [3,4] have a continuous demand for new polymeric materials which exhibit structure on different length scales. These materials must be non-cytotoxic, easy to functionalize, and swell in water [5–7]. Hyperbranched polyglycerol (hPG) combines these properties and is thus useful for many biomedical applications [8–10]. The multivalent hydroxyl functionality of hPG allows its surface to be modified with bioactive substances [11], while the polymer remains water soluble. Moreover, hPG is even less cytotoxic than the structurally similar, well established and FDA-approved polyethylene glycol (PEG) [12–14].

hPG is traditionally prepared by anionic, ring-opening multibranching polymerization of glycidol under slow monomer addition [15,16]. These conditions yield polymers with a narrow polydispersity and a number average molecular weight (M_n) of up to 20 kDa [17]. Recently, Brooks and co-workers reported a molecular weight extension of hPG up to 1 MDa, which corresponds to a hydrodynamic diameter of 10 nm [18]. However, their heterogeneous polymerization conditions yielded rather polydisperse materials. In addition, Hennink and colleagues used hPG macromonomers to prepare cell-laden hydrogels by a free-radical photo-polymerization [19,20]. The same polymerization method was also applied in soft- and photolithography as well as in micromolding to prepare microparticles [21]. However, despite their utility for some applications, hPG macro- and microgels prepared by these methods exhibit a low degree of swelling, which is unfavorable for many biomedical purposes. Hence, new methods are required for the preparation of defined and swollen hPGs on multiple length scales.

Since polymer nanoparticles with sizes between 25 and 100 nm are expected to show efficient endocytosis into cancer cells [22], we developed polyglycerol nanogels in this size range which are synthesized through the use of miniemulsification methods. The crosslinking of both hPG macromonomers and commercial glycerol-based monomers in miniemulsion nanodroplets yields non-cytotoxic nanogels which show excellent cell penetration [23–25]. We also reported the preparation of disulfide-containing polyglycerol nanogels which degrade in the reductive environment of cells. This responsiveness provides the benefit of a controlled intracellular drug release, while the resultant low molecular weight polymer fragments can be cleared by the kidneys [26]. However, miniemulsion techniques are restricted to the production of nanometer-sized particles [27,28]. For tissue engineering applications, microgels with diameters of more than 50 μm are needed because this size is necessary to encapsulate cells [29], thereby serving to engineer the morphology of the desired scaffolds [30]. To template microparticles in this size domain, microfluidic devices have

* Corresponding authors. Tel.: +1 617 496 0586.
E-mail addresses: seiffert@seas.harvard.edu (S. Seiffert), haag@chemie.fu-berlin.de (R. Haag).
[1] Both authors contributed equally to this work.

0142-9612/$ – see front matter © 2010 Elsevier Ltd. All rights reserved.
doi:10.1016/j.biomaterials.2010.10.010

shown great potential [31–33]. Nevertheless, hPGs have not to date been extended to nano- and microgel particles by the combinatorial use of miniemulsion and droplet microfluidic methods.

In this paper, we describe the size extension of hPGs to the nano- and micrometer scale by gelling hPG and, in part, PEG macromonomers in aqueous droplets. We use miniemulsification and microfluidic emulsification to respectively form nano- and micrometer-sized pre-particle droplets and cure these droplets by free-radical crosslinking polymerization of the hPG building blocks and the PEG macro-crosslinkers, as illustrated in Fig. 1. We perform this reaction under mild conditions which allows us to encapsulate living yeast cells into the resultant microgels, thus demonstrating the low cytotoxicity of the hPG material.

2. Methods

2.1. Materials

Acryloyl chloride, Span 80, and $(NH_4)_2S_2O_8$ (APS) were purchased from Fluka. *N*,*N*,*N*′,*N*′-tetramethylethylenediamine (TEMED), p-methoxyphenol, Tween 80, and 3-mercapto-1,2-propanediol (90%) were obtained from Acros Organics. Triton X and paraffin oil were purchased from Sigma Aldrich. ABIL EM 90 was kindly provided by Evonik Industries (Germany). Phosphate Buffered Saline (PBS buffer) was obtained from BioWhittaker®. Dialysis tubes with a molecular weight cutoff of 50 kDa were obtained from Spectrum®.

Miniemulsions with nanometer-sized droplets were prepared using a Sonicator™ from Heat Systems-Ultrasonics, Inc., Model W-220f. Emulsions with micrometer-sized droplets were formed in glass capillary microfluidic devices [33]. Dynamic light scattering measurements were conducted using a NanoDLS particle size analyzer (Brookhaven Instruments). Transmission electron microscopy samples were prepared on carbon coated copper grids by blotting samples in 1% aqueous uranyl acetate and visualizing them with a Philips CM12 electron microscope. Optical and fluorescence micrographs were recorded on a Leica TCS SP5 confocal laser scanning microscope. ^{1}H NMR spectra were recorded on a Bruker AC250 at 250 MHz, using deuterated water and deuterated chloroform as solvents.

hPG with a number average molecular weight (M_n) of 8 kDa and a weight average molecular weight (M_w) of 14.5 kDa ($hPG_{14.5}$) was prepared as reported previously [34]. Following the procedure described by our group [35], $hPG_{14.5}$ was reacted with acryloyl chloride to form a $hPG_{14.5}$ functionalized with 10 acrylate groups ($hPG_{14.5}$Dea). The resultant reactive polymer was stabilized against free-radical polymerization by the addition of 200 ppm p-methoxyphenol. Polyethylene glycol-diacrylate with a molecular weight of 4.6 kDa ($PEG_{4.6}$Dia) was prepared according to a procedure published by Hubbell et al. [36], whereas polyethylene glycol-diacrylate with a molecular weight of 575 Da ($PEG_{0.575}$Dia) was purchased from Sigma Aldrich.

Yeast cells were *Saccharomyces cerevisiae* strain EBY100 [37] and were cultured in liquid YPD medium (10 g L^{-1} yeast extract, 20 g L^{-1} bactopeptone, 20 g L^{-1} dextrose) at 30 °C on an orbital shaker at ~300 rpm. The density matching agent Optiprep (density 1.32 g L^{-1}) was Sigma Aldrich part #D1556. Optiprep is used to increase the density of the YPD solution so that the cells remain suspended during particle formation. 10x YPD was prepared by dissolving 1 g yeast extract, 2 g bactopeptone, and 2 g dextrose in deionized water to a final volume of 10 mL. The solution was heated to completely dissolve reagents and then passed through a 0.2 μm filter.

2.2. Preparation of polyglycerol nanogels

$hPG_{14.5}$Dea (200 mg) and APS (50 mg) dissolved in PBS buffer (0.75 mL) were pre-emulsified under strong stirring in a solution of Span 80 (300 mg) and Tween 80 (100 mg) in cyclohexane (15 mL). After subsequent miniemulsification with a tip sonicator, the emulsion was degassed for 5 min, and a free-radical crosslinking

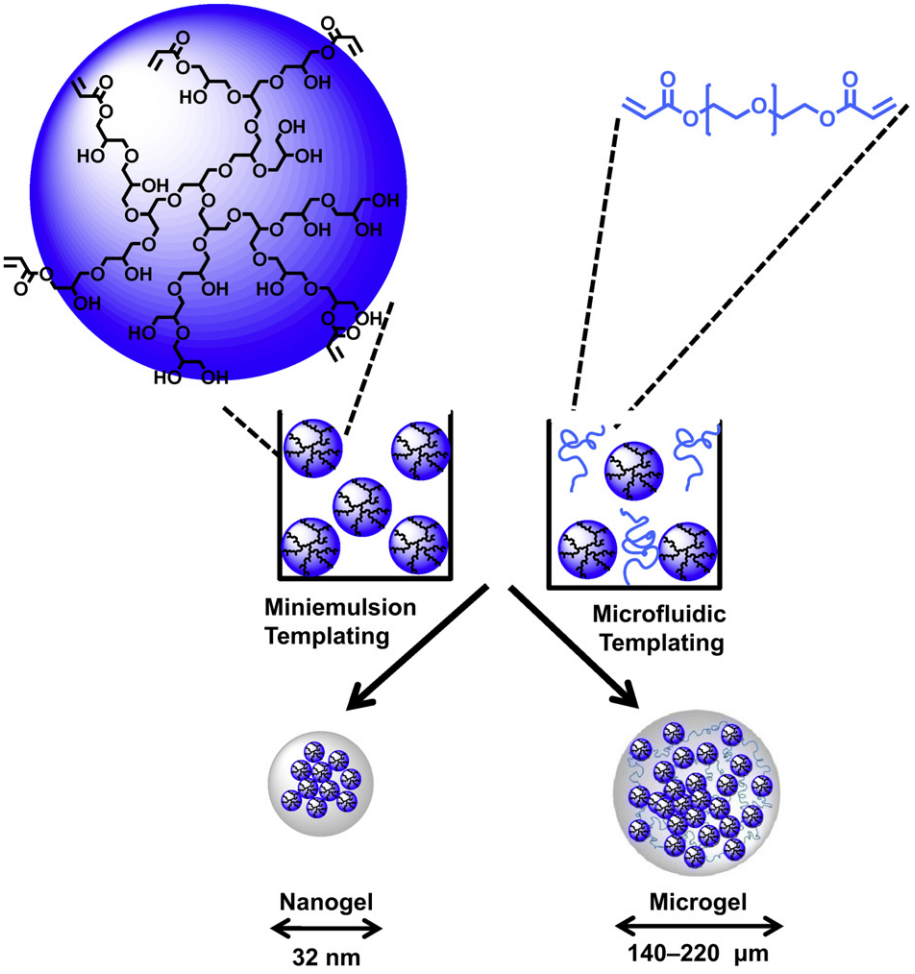

Fig. 1. Schematic of hPG–PEG nano- and microgels obtained by free-radical (co-)polymerization of hyperbranched polyglycerol decaacrylate (dark blue spheres) and polyethylene glycol-diacrylate (light blue lines) in nano- (left) or micrometer-sized (right) pre-gel droplets.

polymerization was initiated by the addition of TEMED to the continuous phase. After 20 min, all remaining acrylate groups on the surface of the resultant nanogels were converted into diols by the addition of 3-mercapto-1,2-propanediol (34.6 μL) and additional APS (50 mg). The hPG nanogels were isolated by diluting the emulsion with cyclohexane (35 mL) and ultracentrifugation (4000 rpm). The nanogels were washed three times with cyclohexane (50 mL) to remove remaining surfactant. A final water dialysis (3 d, 3 solvent exchanges per day, molecular weight cutoff 50 kDa) was performed to remove remaining salts and unreacted 3-mercapto-1,2-propanediol. After water evaporation, about 50% of the hPG nanogels could be recovered.

2.3. Preparation of polyglycerol microgels

For the production of micrometer-sized polyglycerol particles, an hPG–PEG precursor solution was emulsified in glass capillary microfluidic device with a tip diameter of 120 μm. This solution contained a total of 300 g L^{-1} $hPG_{14.5}$Dea, 1 vol.-% $PEG_{0.575}$Dia, and 10 g L^{-1} APS in water. The continuous phase used for the microfluidic emulsification was a mixture of paraffin oil (98 wt.-%) and a modified polyether–polysiloxane surfactant (ABIL EM 90, Evonik Industries, Germany, 2 wt.-%). Pumping these fluids into the microfluidic device with volume flow rates of 0.7 mL h^{-1} for the continuous and 0.3 mL h^{-1} for the dispersed phase led to the formation of ~100 μm droplets of the aqueous phase dispersed in the continuous hydrocarbon phase. The flow rates were adjusted with syringe pumps (Harvard Apparatus, PhD 2000 Series), and analytical glass syringes (Hamilton Gastight) and polyethylene tubing (Scientific Commodities) were used for fluid supply. To monitor the droplet formation, the microfluidic devices were operated on an optical microscope equipped with a digital video camera (Sony XCD-V50). Once formed, the emulsion was stored at 50 °C overnight, thereby gelling the droplets. The resultant microgel particles were transferred into plain water by removing the supernatant organic phase, washing them two times with water plus 0.1 wt-% Triton X to remove the oil phase and four times with plain water to remove the Triton X. After swelling in water, the microgels had a size of 140 μm as confirmed by optical microscopy.

2.4. Preparation and characterization of yeast cell-laden polyglycerol microgels

Yeast cells were cultured in YPD medium overnight, diluted to a concentration of 1.2×10^7 cells·mL^{-1}, and then cultured for 3 h to a concentration of 2.7×10^7 cells·mL^{-1}. Two milliliters of the cell culture were spun in a microfuge for 75 s at 7000 RCF and the pellet was resuspended to approximately 1×10^8 cells·mL^{-1} by addition of 100 μL Optiprep and 400 μL 10x YPD. Then, 3 mg of APS were dissolved in 1 mL of a 600 g L^{-1} $hPG_{14.5}$Dea stock solution, and this solution was combined with 0.4 mL of a 375 g L^{-1} stock solution of $PEG_{4.6}$Dia in water and 0.1 mL of the aqueous yeast cell solution. The resultant cell-laden macromonomer solution, hereinafter referred to as "cell-laden microgel precursor solution", was allowed to sit for about 15 min with occasional shaking, and then emulsified in a glass microcapillary device with a tip diameter of 200 μm. The continuous phase used for the microfluidic emulsification was a mixture of paraffin oil (98 wt.-%) and ABIL EM 90 (2 wt.-%). The fluids were injected with volume flow rates of 1.2 mL h^{-1} for the continuous and 0.4 mL h^{-1} for the dispersed phase, leading to the formation of ~180 μm droplets of the aqueous phase dispersed in the continuous hydrocarbon phase. The flow rates were adjusted with syringe pumps (Harvard Apparatus, PhD 2000 Series), and analytical glass syringes (Hamilton Gastight) and polyethylene tubing (Scientific Commodities) were used for fluid supply. To monitor the droplet formation, the microfluidic devices were operated on an optical microscope equipped with a digital video camera (Sony XCD-V50). After collection, the emulsion was stored at 30 °C overnight, thereby gelling the drops. The resultant cell-laden microgel particles were transferred into plain water by removing the supernatant organic phase, washing them two times with water plus 0.1 wt-% Triton X and four times with plain water, whereupon they swelled to size of 220 μm as confirmed by optical microscopy.

To appraise the elastic modulus of the cell-laden microgels, a macroscopic sample with the same concentration of $hPG_{14.5}$Dea (450 g L^{-1}) and $PEG_{4.6}$Dia (100 g L^{-1}) as used for the cell-laden microgel fabrication was gelled between the plates of rheomoter with a cone–plate geometry (Bohlin Gemini, cone diameter 40 mm, cone angle 4°). During the reaction, the elastic (G') and viscous part (G'') of the complex shear modulus were measured by continuous oscillation at a frequency of 1 Hz, a deformation of 1%, and a temperature of 30 °C. The final plateau value of the elastic modulus, G'_∞, was estimated by fitting the experimental time-dependent modulus $G'(t)$ to a modified Hill function [38], yielding G'_∞(1 Hz, 30 °C) = 2.6 kPa.

2.5. Yeast live–dead assays

To appraise the viability of the yeast cells encapsulated into hPG–PEG microgels, the Invitrogen LIVE/DEAD® FungaLight™ Yeast Viability Kit (L34952) was used. This kit includes the Syto 9® green-fluorescent nucleic acid stain (Ex/Em 480/500 nm), which can penetrate yeast with damaged or intact membranes, and the red-fluorescent nucleic acid stain propidium iodide (Ex/Em 490/635 nm), which can penetrate only yeast with damaged membranes. It is not necessary to wash cells and particles after staining with these dyes. To prepare control samples with dead cells only, yeast cells and gel particles containing yeast cells were pelleted by centrifugation (6000 RCF for 90 s), washed once with 1 mL of 70% ethanol, resuspended in 1 mL of 70% ethanol, and incubated at room temperature for 20 min. These samples were then centrifuged for 90 s at 4000 RCF, washed once with 500 μL deionized water, once with 200 μL deionized water, and resuspended in 200 μL deionized water containing 0.2 μL Syto 9® and 0.2 μL propidium iodide. These samples were incubated for 10 min in the dark at room temperature, and then 10 μL of each was placed on a microscopy slide for analysis by confocal microscopy using a Leica TCS SP5 confocal laser scanning microscope. Fluorescence excitation of the green (Syto 9®) and the red (propidium iodide) dye was performed using the 488-nm line of an Ar ion laser, operating at 4% of its maximum power (6 mW at the object level), and the 543-nm line of an HeNe laser, operating at 50% of its maximum power (0.3 mW at the object level). Fluorescence detection took place in two separate channels in the range of 500–535 nm (green channel) and 558–638 nm (red channel). A third channel was used to obtain a bright field image, and fluorescence and bright field information were overlaid by the Leica software (LAS AF Version 2.1.0 build 4316).

3. Results and discussion

3.1. Fabrication of polyglycerol nanogels

When polymer nano- or microparticles are formed under mild reaction conditions, biologically active species or molecules can be encapsulated without sacrifice of their bioactivity. To take advantage of this feature, we form polyglycerol particles by a free-radical crosslinking polymerization of $hPG_{14.5}$Dea building blocks in nanodroplets. This polymerization can be initiated by a 1:1 M ratio of ammonium persulfate (APS) and *N,N,N′,N′*-tetramethylethylenediamine (TEMED) in aqueous solution at room temperature; moreover, the water-based emulsion templates can be stabilized by bio-inert surfactants such as Span 80 and Tween 80. Both of these experimental features provide mild conditions during the reaction. Besides acting as an initiator, APS serves as an ultralipophobe, thereby stabilizing the miniemulsion by development of an osmotic pressure inside the oil droplets.

With these experimental conditions, we emulsify a solution of $hPG_{14.5}$Dea and APS in PBS buffer (pH 7.4) in a solution of Span 80 and Tween 80 in cyclohexane by rapid stirring. Upon high energy input by a tip sonicator, transparent miniemulsions form and serve as templates for subsequent droplet gelation, as sketched in Fig. 2A. The droplet gelation is achieved by the addition of TEMED to the emulsion: diffusion of TEMED into the miniemulsion droplets catalyzes the decomposition of APS, which triggers the free-radical crosslinking polymerization of the $hPG_{14.5}$Dea building blocks inside the drops. To prevent uncontrolled nanogel growth and macrogel formation, remaining acrylate groups are converted into diols by the addition of thioglycerol, as confirmed by subsequent ^{1}H NMR analysis. After extensive washing and dialysis, we obtain polyglycerol nanogels which exhibit an average diameter of 32 nm with a standard deviation of ±3.8 nm, as determined by dynamic light scattering (DLS). By contrast, transmission electron microscopy (TEM) reveals a significantly smaller average diameter of 23 nm with a standard deviation of ±4.9 nm, as shown in Fig. 2B. Since DLS probes the nanogel diameter in the swollen state whereas TEM visualizes the dry nanogels, the difference between these two values indicates the degree of swelling of the nanogels in aqueous solution, which is 270% (v/v).

3.2. Fabrication of polyglycerol microgels and yeast cell encapsulation

To extend the size of hPG to the micrometer range, we use microfluidic devices to form monodisperse microdroplets as templates for the particle syntheses. We assemble these devices from glass microcapillaries [33]. A typical device with a capillary tip diameter of 120 μm is shown in Fig. 2C. When this device is operated with an aqueous phase that consists of the reactive

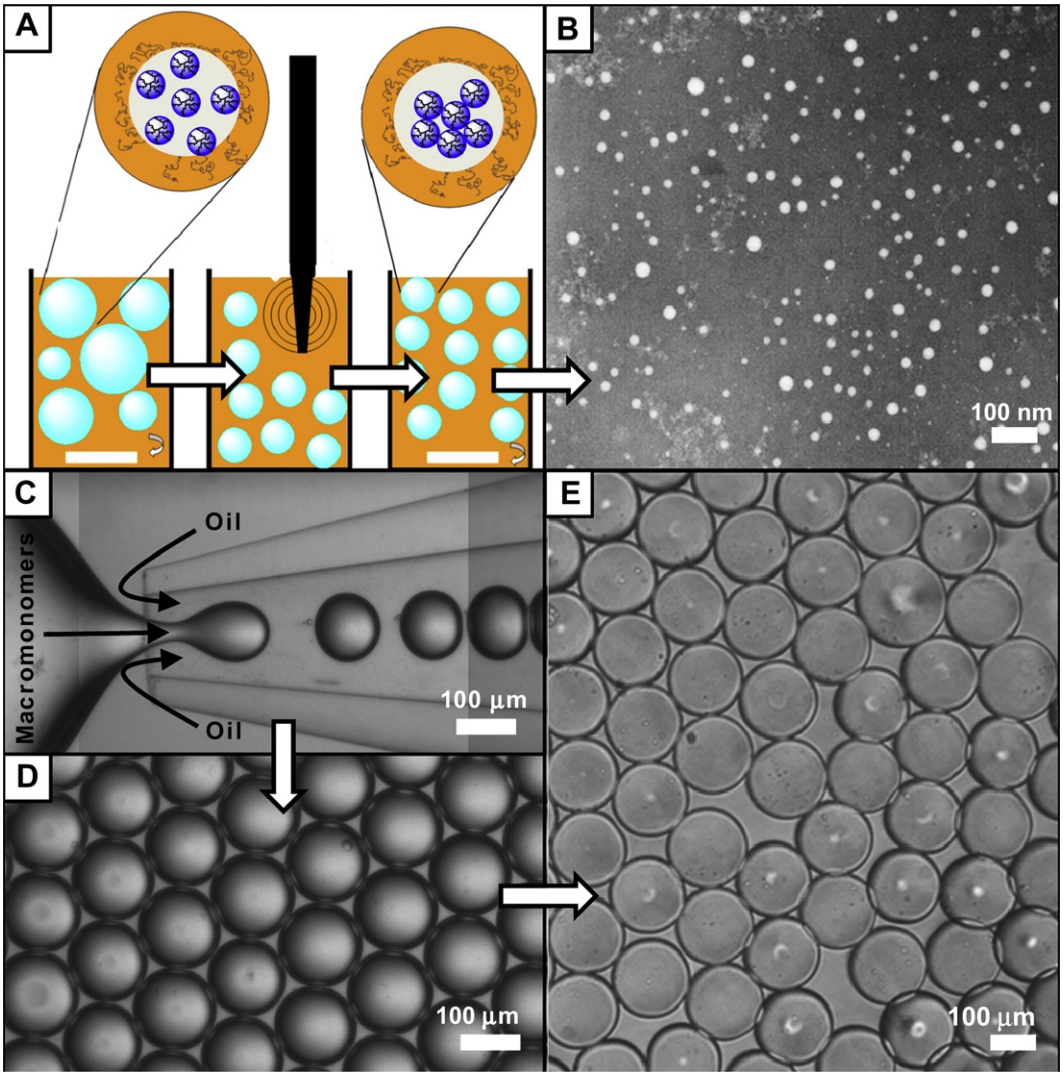

Fig. 2. Fabrication of hPG–PEG nano- and microgel particles. (A) Miniemulsion templating of nanometer-sized droplets (turquoise spheres) that are loaded with hyperbranched polyglycerol decaacrylate (blue spheres). (B) TEM micrograph of nanogel particles obtained by gelation of these nanodroplets. (C) Droplet microfluidic templating of similar, micrometer-sized droplets using a glass microcapillary device. (D) Pre-microgel emulsion obtained from the experiment in Panel C. (E) Optical micrograph of water-swollen microgel particles formed by gelation of the droplets in Panel D.

macromonomers $hPG_{14.5}$Dea and $PEG_{0.575}$Dia as well as the initiator APS, we obtain monodisperse pre-microgel water-in-oil emulsion droplets with diameters of 100 µm, as shown in Fig. 2C and D. These droplets are collected and gelled by subsequent copolymerization of the macromonomers. In a typical experiment, we cure them by overnight storage at 50 °C and transfer the resultant hPG–PEG microgels into water, where they swell to a uniform size of 140 µm, as analyzed with an optical microscope and shown in Fig. 2E. Similar microgels can also be formed with milder reaction conditions: instead of curing the templating emulsion droplets at 50 °C, we can also use a polymerization temperature of only 30 °C, which is still sufficient to form microgel particles.

Since the hPG building blocks are non-cytotoxic [12–14] and easy to functionalize [11], they hold promise to be used as scaffolds for the synthesis of cell-laden microparticles. To produce such particles, we suspend living yeast cells in an aqueous precursor phase which consists of $hPG_{14.5}$Dea and $PEG_{4.6}$Dia. The precursor phase also contains the initiator APS at a concentration which is now lowered to only 2 g L^{-1} to prevent excessive formation of free radicals. We then apply the microfluidic approach to form monodisperse pre-microgel droplets and use mild polymerization conditions of 30 °C to cure these droplets. The resultant microgels are highly loaded with yeast cells which strongly agglomerate in the particles, as shown in Fig. 3A. After gelation of the precursor droplets, these encapsulated cells are immobile and unable to increase significantly in size, because the surrounding polymer gel exhibits an elastic modulus in the range of a few kilopascals, as determined by oscillatory shear rheology on a macroscopic control sample, thereby preventing significant cell movement and expansion. As a result *S. cerevisiae* cells, which must grow to a critical size before they enter the cell cycle [39], are unlikely to divide in these particles. Nevertheless, the polymer matrix allows the cells to metabolize, and hence, a marked percentage of the cells stay alive for more than 12 h after the particle formation.

To investigate the viability of the encapsulated cells, we perform a live–dead assay. Roughly 30% of the cells that were encapsulated into fully polymerized particles are labeled with Syto 9®, which stains live and dead cells green, but not by propidium iodide, which stains only dead cells red (Fig. 3A, zoom-in). Hence, about 30% of the cells that were encapsulated into the microgel particles stay alive after microgel gelation. In a control experiment, treatment of the yeast-containing particles with 70% ethanol prior to staining

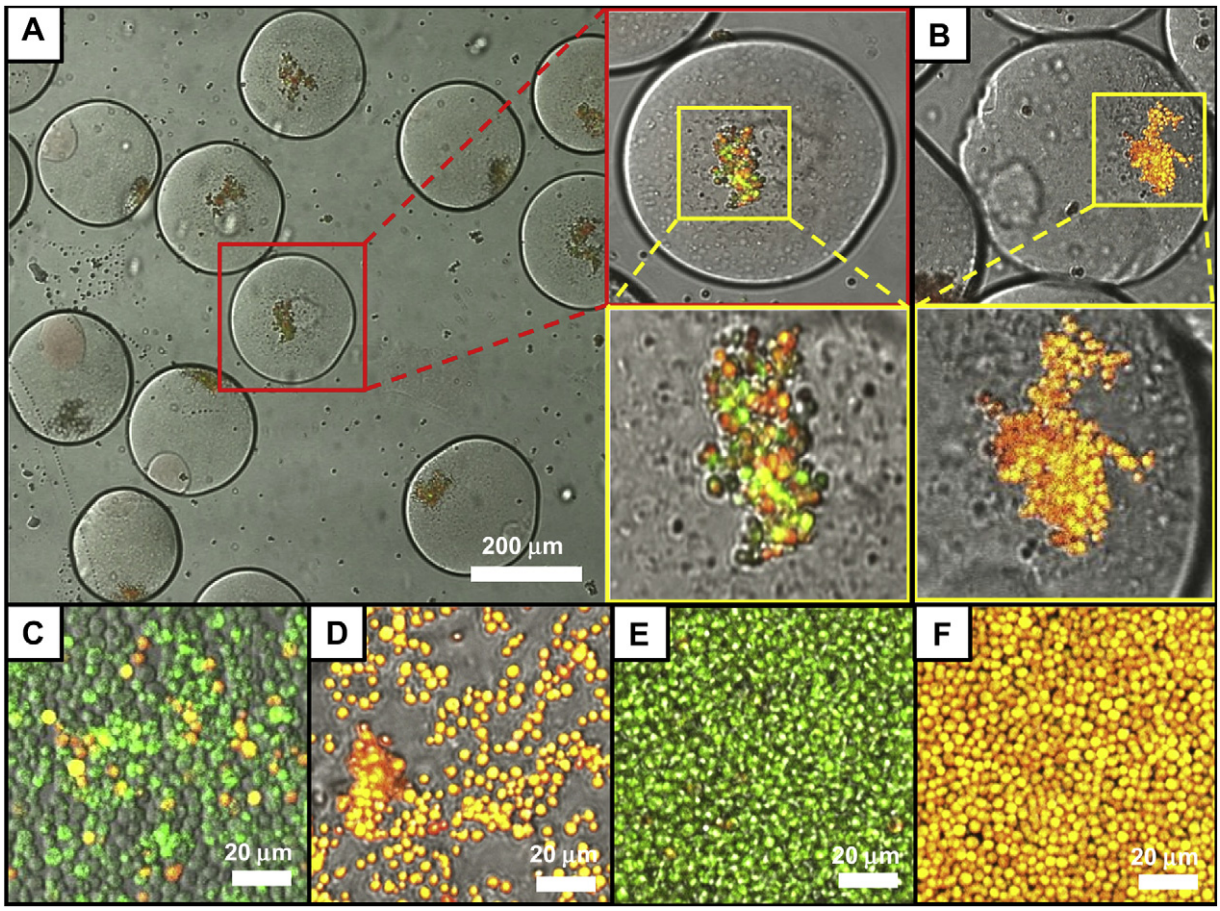

Fig. 3. Viability of yeast cells encapsulated into hPG–PEG microgels. The samples were stained with Syto 9® (green dye, staining both living and dead cells) and propidium iodide (red dye, staining dead cells only) and then observed by bright field and confocal fluorescence microscopy. Green staining denotes living cells, whereas red or yellow staining marks dead cells. (A) Yeast cells encapsulated into hPG–PEG microgels which were gelled overnight at 30 °C. (B) Same particles after treatment with 70% ethanol to kill all encapsulated cells prior to staining. (C) Microgel precursor mixture, comprised of yeast cells and all components required to make hPG–PEG microgels, but incubated overnight at room temperature instead of 30 °C, and hence, not gelled. (D) Microgel precursor mixture after treatment with 70% ethanol prior to staining. (E) Living yeast cells, diluted to 0.5×10^7 cells·mL^{-1} in YPD and cultured overnight at 30 °C. (F) Cell solution from Panel E after treatment with 70% ethanol prior to staining.

causes all cells to be strongly stained by propidium iodide, as demonstrated in Fig. 3B. This observation confirms that the green cells in Fig. 3A are alive and able to exclude the red dye.

When cells are incubated overnight in the cell-laden microgel precursor solution at room temperature, the initiator is significantly less active than it is at 30 °C; hence, free radicals do not form to an extent as they do at 30 °C, and the solution remains liquid. Under these conditions, about 80% of the cells remain viable, as shown in Fig. 3c and d. This finding suggests that the primary cause of cell death during gel encapsulation is the activated initiator or the free radicals it produces, but not the presence of the hPG material, which is thus proven to be reasonably non-cytotoxic. If cells are grown overnight to saturation ($\sim 1.2 \times 10^8$ cells·mL^{-1}) in YPD, virtually all cells are viable and able to exclude propidium iodide, as demonstrated in Fig. 3E and F.

Fedorovich and co-workers obtained a multipotent stromal cell viability of 75% upon encapsulation of the cells into a hPG hydrogel by photoinitiated free-radical polymerization [19]. Even though the comparison of two different cell lines is critical, our approach yields a significantly lower cell viability of only 30%. However, as cell incubation with our hPG-Dea starting materials shows a very high cell viability of 80%, we conclude that hPG by itself is an excellent building block for cell-laden microgels. Consequently, we plan to investigate more bioorthogonal gelation reactions using hPG building blocks in the future.

4. Conclusion

We have extended hyperbranched polyglycerols to nano- and microgel particles. The use of a free-radical polymerization of $hPG_{14.5}Dea$ in miniemulsion droplets, initiated by APS/TEMED, yields defined nanogels with a mean hydrodynamic diameter of 32 nm. By extension of this method to the use of micrometer-sized droplets, as obtained through microfluidic emulsification, we are able to form monodisperse hPG microgels with uniform diameters of several tens or hundreds of micrometers. These microgels form at very mild polymerization condition and can thus be used for the encapsulation of yeast cells, which show a cell viability of about 30%. To further decrease the cytotoxicity of the particle synthesis, our ongoing work focuses on approaches which involve a bioorthogonal coupling of the hPG building blocks without the need for free radicals.

Acknowledgements

We thank Eric V. Shusta (Department of Chemical and Biological Engineering, University of Wisconsin–Madison, Madison, WI 53706, USA) for providing the Yeast strain EBY100. We also thank Svenja Grube (Institute of Physical Chemistry, Clausthal University of Technology, D-38678 Clausthal-Zellerfeld, Germany) for her help with macrogel rheology, as well as Andrea Schulz (Institute for

Chemistry and Biochemistry, Free University Berlin, D-14195 Berlin, Germany) for TEM measurements. This work was supported by the NSF (DMR-1006546), the Harvard MRSEC (DMR-0820484), the German Research Foundation (DFG, SFB 765), and the German Federal Ministry of Education and Research (Poly4Bio). S.S. is a research fellow of the German Academy of Sciences Leopoldina (BMBF-LPD 9901/8-186).

Appendix

Figures with essential color discrimination. All figures in this article are difficult to interpret in black and white. The full color images can be found in the online version, at doi:10.1016/j.biomaterials.2010.10.010.

References

[1] Haag R, Kratz F. Polymer therapeutics: concepts and applications. Angew Chem Int Ed Engl 2006;45(8):1198–215.
[2] Duncan R. Polymer conjugates as anticancer nanomedicines. Nat Rev Cancer 2006;6(9):688–701.
[3] Bettinger CJ, Langer R, Borenstein JT. Engineering substrate topography at the micro- and nanoscale to control cell function. Angew Chem Int Ed Engl 2009;48(30):5406–15.
[4] Langer R. Biomaterials in drug delivery and tissue engineering: one laboratory's experience. Acc Chem Res 2000;33(2):94–101.
[5] Huebsch N, Mooney DJ. Inspiration and application in the evolution of biomaterials. Nature 2009;462(7272):426–32.
[6] Ratner BD, Bryant SJ. Biomaterials: where we have been and where we are going. Annu Rev Biomed Eng 2004;6:41–75.
[7] Langer R, Tirrell DA. Designing materials for biology and medicine. Nature 2004;428(6982):487–92.
[8] Wilms D, Stiriba SE, Frey H. Hyperbranched polyglycerols: from the controlled synthesis of biocompatible polyether polyols to multipurpose applications. Acc Chem Res 2010;43(1):129–41.
[9] Calderon M, Quadir MA, Strumia M, Haag R. Functional dendritic polymer architectures as stimuli-responsive nanocarriers. Biochimie 2010;92(9):1242–51.
[10] Calderon M, Quadir MA, Sharma SK, Haag R. Dendritic polyglycerols for biomedical applications. Adv Mater 2010;22(2):190–218.
[11] Calderon M, Graeser R, Kratz F, Haag R. Development of enzymatically cleavable prodrugs derived from dendritic polyglycerol. Bioorg Med Chem Lett 2009;19(14):3725–8.
[12] Khandare J, Mohr A, Calderon M, Welker P, Licha K, Haag R. Structure-biocompatibility relationship of dendritic polyglycerol derivatives. Biomaterials 2010;31(15):4268–77.
[13] Kainthan RK, Hester SR, Levin E, Devine DV, Brooks DE. In vitro biological evaluation of high molecular weight hyperbranched polyglycerols. Biomaterials 2007;28(31):4581–90.
[14] Kainthan RK, Brooks DE. In vivo biological evaluation of high molecular weight hyperbranched polyglycerols. Biomaterials 2007;28(32):4779–87.
[15] Sunder A, Mulhaupt R, Haag R, Frey H. Hyperbranched polyether polyols: a modular approach to complex polymer architectures. Adv Mater 2000;12(3):235–9.
[16] Sunder A, Hanselmann R, Frey H, Mulhaupt R. Controlled synthesis of hyperbranched polyglycerols by ring-opening multibranching polymerization. Macromolecules 1999;32(13):4240–6.
[17] Wilms D, Wurm F, Nieberle J, Bohm P, Kemmer-Jonas U, Frey H. Hyperbranched polyglycerols with elevated molecular weights: a facile two-step synthesis protocol based on polyglycerol macroinitiators. Macromolecules 2009;42(9):3230–6.
[18] Kainthan RK, Muliawan EB, Hatzikiriakos SG, Brooks DE. Synthesis, characterization, and viscoelastic properties of high molecular weight hyperbranched polyglycerols. Macromolecules 2006;39(22):7708–17.
[19] Fedorovich NE, Oudshoorn MH, van Geemen D, Hennink WE, Alblas J, Dhert WJA. The effect of photopolymerization on stem cells embedded in hydrogels. Biomaterials 2009;30(3):344–53.
[20] Oudshoorn MHM, Rissmann R, Bouwstra JA, Hennink WE. Synthesis and characterization of hyperbranched polyglycerol hydrogels. Biomaterials 2006;27(32):5471–9.
[21] Oudshoorn MHM, Penterman R, Rissmann R, Bouwstra JA, Broer DJ, Hennink WE. Preparation and characterization of structured hydrogel microparticles based on cross-linked hyperbranched polyglycerol. Langmuir 2007;23(23):11819–25.
[22] Zhang SL, Li J, Lykotrafitis G, Bao G, Suresh S. Size-dependent endocytosis of nanoparticles. Adv Mater 2009;21(4):419–24.
[23] Sisson AL, Steinhilber D, Rossow T, Welker P, Licha K, Haag R. Biocompatible functionalized polyglycerol microgels with cell penetrating properties. Angew Chem Int Ed Engl 2009;48(41):7540–5.
[24] Sisson AL, Papp I, Landfester K, Haag R. Functional nanoparticles from dendritic precursors: hierarchical assembly in miniemulsion. Macromolecules 2009;42(2):556–9.
[25] Sisson AL, Haag R. Polyglycerol nanogels: highly functional scaffolds for biomedical applications. Soft Matter 2010;6(20):4968–75.
[26] Steinhilber D, Sisson AL, Mangoldt D, Welker P, Licha K, Haag R. Synthesis, reductive cleavage, and cellular interaction studies of biodegradable, polyglycerol nanogels. Adv Funct Mater; 2010. doi:10.1002/adfm.201000410.
[27] Landfester K. Miniemulsion polymerization and the structure of polymer and hybrid nanoparticles. Angew Chem Int Ed Engl 2009;48(25):4488–507.
[28] Antonietti M, Landfester K. Polyreactions in miniemulsions. Prog Polym Sci 2002;27(4):689–757.
[29] Panda P, Ali S, Lo E, Chung BG, Hatton TA, Khademhosseini A, et al. Stop-flow lithography to generate cell-laden microgel particles. Lab Chip 2008;8(7):1056–61.
[30] Khademhosseini A, Langer R, Borenstein J, Vacanti JP. Microscale technologies for tissue engineering and biology. Proc Natl Acad Sci U S A 2006;103(8):2480–7.
[31] Tumarkin E, Kumacheva E. Microfluidic generation of microgels from synthetic and natural polymers. Chem Soc Rev 2009;38(8):2161–8.
[32] Teh SY, Lin R, Hung LH, Lee AP. Droplet microfluidics. Lab Chip 2008;8(2):198–220.
[33] Shah RK, Kim JW, Agresti JJ, Weitz DA, Chu LY. Fabrication of monodisperse thermosensitive microgels and gel capsules in microfluidic devices. Soft Matter 2008;4(12):2303–9.
[34] Haag R, Mecking S, Türk H. DE 10211664A1; 2002.
[35] Ricken S, Osinski PW, Eilbracht P, Haag R. A new approach to dendritic supported nixantphos-based hydroformylation catalysts. J Mol Catal A Chem 2006;257(1–2):78–88.
[36] Elbert DL, Pratt AB, Lutolf MP, Halstenberg S, Hubbell JA. Protein delivery from materials formed by self-selective conjugate addition reactions. J Control Release 2001;76(1–2):11–25.
[37] Boder ET, Wittrup KD. Yeast surface display for screening combinatorial polypeptide libraries. Nat Biotechnol 1997;15(6):553–7.
[38] Oppermann W, Okay O. Polyacrylamide–clay nanocomposite hydrogels: rheological and light scattering characterization. Macromolecules 2007;40(9):3378–87.
[39] Jorgensen P, Nishikawa JL, Breitkreutz BJ, Tyers M. Systematic identification of pathways that couple cell growth and division in yeast. Science 2002;297(5580):395–400.